



Modeling of the kinetics of pervaporative recovery of ethanol from fermented broth with the use of the solution–diffusion theory

Marek Staniszewski^{a*}, Wojciech Kujawski^b

^aFaculty of Food Science, University of Warmia and Mazury, pl. Cieszyński 1, 10–726 Olsztyn, Poland

Tel.: +48 895233510; Fax: +48 895233402; email: msta@uwm.edu.pl

^bNicolaus Copernicus University, Faculty of Chemistry, Membrane Separation Processes Group, ul. Gagarina 7, 87-100 Toruń, Poland

Received 3 July 2009; accepted 26 August 2009

ABSTRACT

The aim of this study was a mathematical description of the kinetics of ethanol separation from fermentation broth of *Saccharomyces cerevisiae* yeast by the vacuum pervaporation technique. Model equations were developed on basis of the solution–diffusion theory. The finite differences method has been used to calculate the concentration profiles of permeants within the membrane. The optimal number of grid points and their distances were found by numerical tests. The formulated model describes the transport of feed components under the non-stationary conditions. Model equations were solved with the use of the backward differentiation method. Model parameters were estimated by fitting of experimental data with the use of the Nelder–Mead method. Calculations were performed for separation experiments with broths containing 3–6 wt% of ethanol. Very good agreement with the experimental data was obtained.

Keywords: Solution–diffusion model; Pervaporation; Kinetics of separation; Ethanol; Broth

1. Introduction

Pervaporation is a membrane separation technique, which is generally applied to separate liquid mixtures [1–3]. Due to the mechanism of separation, this technique can be also employed to the ethanol removal from the post-fermentation liquid. In this method, the feed is located on one side of the non-porous hydrophobic membrane. The permeate side is kept either under the vacuum (vacuum pervaporation) or is swept with a stream of an inert gas (sweeping gas pervaporation) [1–3].

The aim of this work was design of a kinetic model of ethanol recovery by the vacuum pervaporation with the use of the solution–diffusion theory and applying

them for describing of the product separation from fermented broth of *Saccharomyces cerevisiae* yeast.

2. Modeled system

2.1. Fermentation

In the investigated system ethanol was produced in a bioreactor from lactose with the use of co-immobilized β -galactosidase and yeast cells (*S. cerevisiae*). The details of biocatalyst preparation and fermentation procedure have been published by Lewandowska and Kujawski [4]. The dried whey permeate supplemented with growth factors was used as a substrate for fermentation. The process was carried out in a semi-continuous mode, i.e. with periodical supplying of substrate and removal of a part of fermented broth. In this system the maximal ethanol content

*Corresponding author

reached in bioreactor (6 wt%) is limited due to glucose repression and inhibitory effect of accumulation of dead cells in biocatalyst [5].

2.2. Ethanol separation

The ethanol produced in a bioreactor was recovered from the broth by pervaporation. The experiments were carried out with the use of a laboratory pervaporation unit working in a vacuum pervaporation mode. A composite membrane PDMS-PAN (Pervatech B.V., the Netherlands) was used. The separation ability of this membrane determines skin layer made of polydimethylsiloxane (PDMS) [6]. The hydrophobic character of this polymer causes preferential transport of ethanol and offers possibility of its separation from mixtures of composition close to that produced in ethanolic fermentation. The scheme and the detailed description of the fermentation/pervaporation system used for ethanol production has been presented elsewhere [4].

3. Theory

3.1. Solution–diffusion–permeation model

The solution–diffusion model is one of widely applied models for describing of mass transport in polymeric materials. This model, designed originally to explain the transport of gases through polymeric films, has been adapted for membrane separation processes and is used in modeling of such techniques as reverse osmosis [7,8], nanofiltration [9,10], gas separation [11,12] and pervaporation [13,14].

The theory of transport occurred by solution–diffusion mechanism presented by Lonsdale et al. [15] is based on the assumption that flux of each permeant is described by the first Fick's law.

$$J_i = -\rho_m D_i (w_1^m, w_2^m, \dots, w_n^m) \frac{dw_i^m}{d\delta} \quad (1)$$

In Eq. (1): J_i – flux, D_i – diffusion coefficient of permeant, δ – thickness of a membrane, ρ_m – density, w_i^m – weight fraction of component within a membrane. Detailed solution of Eq. (1) depends on membrane properties and boundary conditions.

To describe the mass transport through a non-porous polymeric membrane from binary mixtures de Pinho et al. [16] proposed a model in which diffusion coefficients of permeants are dependent on concentrations of both components by an exponential-type expression, i.e.

$$D_i = D_{i,0} \exp(\tau_{ii} w_i^m + \tau_{ij} w_j^m) \quad (2)$$

$$D_j = D_{j,0} \exp(\tau_{ji} w_i^m + \tau_{jj} w_j^m) \quad (3)$$

Parameters τ_{ij} describe interactions between components and a membrane. It is assumed, that sorption of component i within a membrane at feed side depends on sorption coefficient of a pure component in polymer $\phi_{i,f}$ and is a linear function of the permeant mole fraction in a feed $x_{i,f}$.

$$w_i^m = \phi_{i,f} \gamma_{i,f} x_{i,f} \quad (4)$$

Integration of Eqs. (2) and (3) over membrane thickness while neglecting the permeant activity at permeate side gives the equation for the flux of water (Eq. 5).

$$J_i = \rho_m \frac{D_{i,0}}{\delta \tau_{ii}} [\exp(\tau_{ii} w_i^m) - 1] \quad (5)$$

For binary systems, the ratio of water flux and the second (organic) component flux q is expressed as

$$q = \frac{\tau_{ii} D_{i,0} [\exp((\tau_{ii} - \tau_{ji}) w_i^m) - 1]}{(\tau_{ii} - \tau_{ji}) D_{j,0} [\exp(\tau_{jj} w_j^m) - 1]} \quad (6)$$

De Pinho's model is derived for transport from a binary feed solutions occurring at stationary conditions, i.e. at constant composition of the feed. The use of this model needs the evaluation of five parameters on basis of transport experiments performed for different feed compositions.

3.2. Model for non-stationary conditions

On the basis of the theory presented above the model for non-stationary transport of components from feed has been worked out. To solve mass transport equations within the membrane the finite differences method [17] has been used.

The following assumptions have been made. Local flux of permeant A in the inside of membrane depends on local concentrations of all permeants within a membrane, and is expressed by Eq. (7).

$$J_{A,i} = -P_A \left(\frac{C_{A,i+1} - C_{A,i}}{l} \right) \frac{1}{2} (\tau_A (C_{A,i} + C_{A,i+1}) + \tau_{AB} (C_{B,i} + C_{B,i+1})) \quad (7)$$

In Eq. (7): P_A – a permeability coefficient of component A , $C_{A,i}$ and $C_{A,i+1}$ – concentrations of compounds

A at points $i, i+1, l$ – grid points distance, τ_A – a plasticization coefficient of the component A, and τ_{AB} – a coupled plasticization coefficient of component A enhanced by the presence of component B. $J_{A,i}$ is the flux of component A within a membrane from the grid point of index i to point of index $i+1$. Point with an index “1” corresponds to the membrane surface at feed side. For the permeant B, the equation for the flux is following:

$$J_{B,i} = -P_B \left(\frac{C_{B,i+1} - C_{B,i}}{l} \right) + \frac{1}{2} (\tau_B (C_{B,i} + C_{B,i+1}) + \tau_{BA} (C_{A,i} + C_{A,i+1})) \quad (8)$$

In Eq. (8): τ_B is a plasticization coefficient of component B, τ_{BA} – a coupled plasticization coefficient of component B. Permeability coefficients P_A, P_B (Eqs. (7) and (8)) are defined as products of corresponding partition coefficients k_A, k_B and diffusion coefficients D_A, D_B .

$$P_A = k_A D_A \quad (9)$$

$$P_B = k_B D_B \quad (10)$$

Partition coefficients k_A, k_B describe equilibrium sorption of components to the membrane at feed side.

$$k_A = \frac{C_{A,1}}{C_{A,f}} \quad (11)$$

$$k_B = \frac{C_{B,1}}{C_{B,f}} \quad (12)$$

System of equations describing concentration profiles of components diffusing across membrane is obtained by combining Eqs. (7) and (8) for each grid point. The optimal number of grid points and their distances were found by numerical tests in order to maximizing accuracy of approximation and efficiency of calculations.

The composition of a feed is time-related due to differences in the rate of permeation of components. Masses of components in feed m_A, m_B during separation decrease with the rate dependent on the actual permeation rate of a component (Eqs. (13)–(14)).

$$\frac{dm_A}{dt} = -J_{A,0} A_m \quad (13)$$

$$\frac{dm_B}{dt} = -J_{B,0} A_m \quad (14)$$

J_0 is the flux of a component from the feed into a membrane, A_m – the area of a membrane. It is assumed that at permeate side $C_{A,p} = 0$ and $C_{B,p} = 0$.

The system of time-related differential equations which describes the changes of feed composition and accumulation of permeants within a membrane was solved with the use of the backward differentiation method [17]. The advantage of this method is that only kinetics data are required for identifying the parameters of the presented model. Therefore the additional sorption measurements are not needed.

3.3. Indices of separation performance

Selectivity coefficient α is defined as a ratio of fluxes of permeating components J_{EtOH}, J_{water} (Eq. (15)).

$$\alpha = \frac{J_{EtOH}}{J_{water}} \quad (15)$$

The recovery coefficient D_r of ethanol is calculated from Eq. (16)

$$D_r = \frac{m_0 - m_t}{m_0} \quad (16)$$

where: m_0 – the initial mass of ethanol in a feed, m_t – the mass of ethanol after time t .

3.4. Evaluation of model parameters

Unknown model parameters, i.e. $P_A, \tau_A, \tau_{AB}, P_B, \tau_B, \tau_{BA}$, have been found by direct fitting of relationship $D_r = f(t)$ by using model equations (Eqs. (7), (8), (13) and (14)) and kinetics data collected during separation of ethanol from broth. The Nelder–Mead method was used for the best fitting [18]. This method is one of non-gradient optimization techniques for finding a local minimum of a function – only evaluations of the objective function at vertices of a simplex are used.

The minimized function F was a sum of squared residuals between values of recovery coefficients D_r determined experimentally and predicted by the model (Eq. (17)).

$$F = \sum_{i=1}^n \left(Y_i^{(e)} - Y_i^{(m)} \right)^2 \quad (17)$$

In Eq. (17): $Y_i^{(e)}$ is an experimental value, $Y_i^{(m)}$ – a value predicted by model, n – a number of observations. The search of minimum was terminated when the standard deviation of the objective function F calculated for each vertex of simplex dropped below a pre-set value ε (Fig. 1).

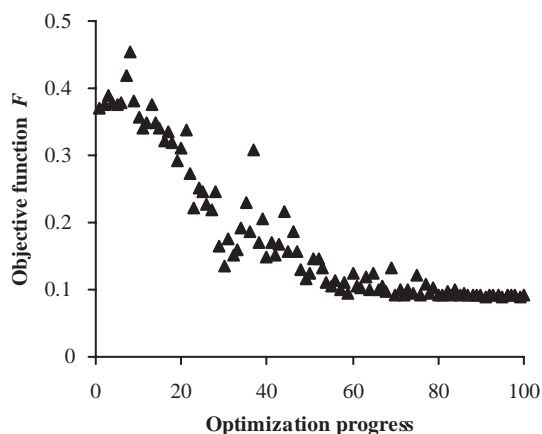


Fig. 1. Evaluation of the model parameters by the Nelder–Mead algorithm with data obtained in 4th cycle of fermentation.

$$\sum_{i=0}^n \sqrt{\frac{(F_i - F_{\text{avg}})^2}{n}} < \varepsilon \quad (18)$$

In Eq. (18): n is a number of searched parameters, F_{avg} – an average value of the function.

To check the importance of coupled plasticization coefficients for the kinetics of separation test calculations have been performed for the following assumptions:

- $\tau_{AB} = \tau_{BA} = 0$,
- $\tau_{AB} = \tau_{BA} \neq 0$,
- $\tau_{AB} \neq 0, \tau_{BA} \neq 0$.

The results, obtained during this phase of studies, proved that the last assumption offers the best values

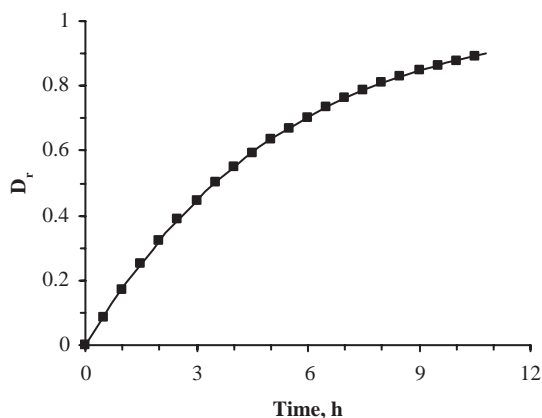


Fig. 2. Kinetics of the ethanol separation from broth produced after 2nd cycle of fermentation. Feed weight: 1,930 g, ethanol content: 4.97 wt%; $R^2 = 0.999988$, RPDM = 0.45%. The solid line represents model predictions.

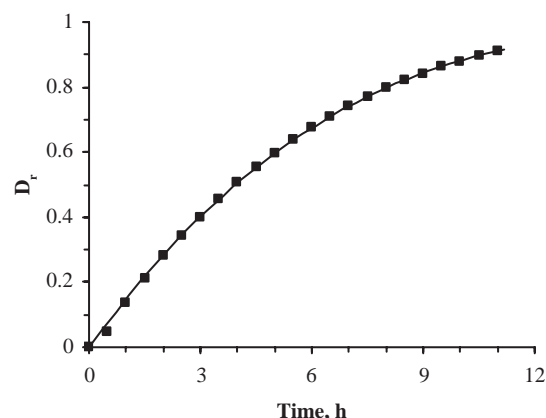


Fig. 3. Kinetics of the ethanol separation from broth produced after 5th cycle of fermentation. Feed weight: 2,000 g, ethanol content: 5.37 wt%; $R^2 = 0.999822$, RPDM = 3.82%.

of the objective function F at the end of optimization procedure with the same value of ε . Therefore, final calculations have been performed taking into account two coupled plasticization coefficients τ_{AB}, τ_{BA} . Values of the estimated parameters, applied as a starting data for the Nelder–Mead algorithm, were the same in all calculations. This procedure was repeated for each separation kinetics. Very good fits have been obtained for all experiments confirming the rightness of the model assumptions. Correlation coefficients varied starting from $R^2 = 0.999988$ for the best fit (Fig. 2) to $R^2 = 0.999822$ for the worst one (Fig. 3).

4. Results and discussion

The set of model parameters found for successive experiments of ethanol separation from the broth have been shown in Table 1. Mean values calculated for these data are following: $P_{A,\text{avg}} = 1.36 \pm 0.61 \text{ cm}^2 \cdot \text{h}^{-1}$, $P_{B,\text{avg}} = 34.0 \pm 2.0 \text{ cm}^2 \cdot \text{h}^{-1}$, $\tau_{A,\text{avg}} = 1.93 \pm 0.68 \text{ cm}^3 \cdot \text{mol}^{-1}$, $\tau_{B,\text{avg}} = 0.09 \pm 0.12 \text{ cm}^3 \cdot \text{mol}^{-1}$, $\tau_{AB,\text{avg}} = 1.72 \pm 0.09 \text{ cm}^3 \cdot \text{mol}^{-1}$, $\tau_{BA,\text{avg}} = 0.99 \pm 0.04 \text{ cm}^3 \cdot \text{mol}^{-1}$.

According to the solution–diffusion theory, the separation ability of a membrane is dominated by both sorption and diffusion of the individual components. The commercial PDMS-PAN membrane is a composite membrane formed by coating of a poly(dimethylsiloxane) film on a porous poly(acrylonitrile) support. The cross-linking degree influences on the transport properties of the membrane by changing of the swelling of PDMS. High permeability of membranes made of this polymer results from very flexible polymer chains. The bonds Si–O–Si forming a backbone are characterized by long bond lengths and high freedom of rotation. The facilitated motion of chain segments leads to an

Table 1
Parameters of model calculated for separation of ethanol from broths produced in successive cycles of the fermentation (A-water, B-ethanol)

Time of fermentation, h	24	48	72	96	120	144	168	192	216	240
Ethanol content, %	3.26	4.97	5.40	4.53	5.37	6.19	5.22	4.28	3.42	2.98
$P_A \pm s^*$	2.32±0.0044	0.71±0.0057	0.89±0.0067	2.38±0.0125	1.21±0.0045	1.47±0.0053	0.94±0.0058	0.86±0.0057	1.05±0.0026	1.81±0.0022
$P_B \pm s^*$	36.9±0.0161	36.3±0.0079	36.2±0.0227	35.8±0.0350	32.2±0.0086	31.5±0.0247	32.6±0.0181	32.4±0.0311	33.0±0.0211	33.1±0.0116
$\tau_A \pm s^{**}$	0.604±0.0015	0.887±0.0088	1.875±0.0014	1.659±0.0026	2.527±0.0010	2.501±0.0020	2.404±0.0032	2.333±0.0081	2.312±0.0025	2.167±0.0009
$\tau_B \pm s^{**}$	0.012±0.0006	0.331±0.0019	0.010±0.0001	0.015±0.0004	0.217±0.0009	0.223±0.0011	0.019±0.0013	0.011±0.0005	0.012±0.0003	0.027±0.0010
$\tau_{AB} + s^{**}$	1.767±0.0016	1.529±0.0015	1.653±0.0007	1.634±0.0028	1.772±0.0018	1.783±0.0021	1.770±0.0030	1.771±0.0011	1.775±0.0019	1.771±0.0009
$\tau_{BA} + s^{**}$	1.000±0.0004	1.024±0.0004	0.900±0.0009	0.947±0.0006	0.999±0.0002	1.018±0.0003	0.997±0.0005	0.996±0.0009	0.998±0.0003	0.999±0.0002
R^2	0.999948	0.999988	0.999870	0.999838	0.999822	0.999834	0.999908	0.999876	0.999954	0.999901

* Expressed in $\text{cm}^2 \cdot \text{h}^{-1}$

** Expressed in $\text{cm}^3 \cdot \text{mol}^{-1}$

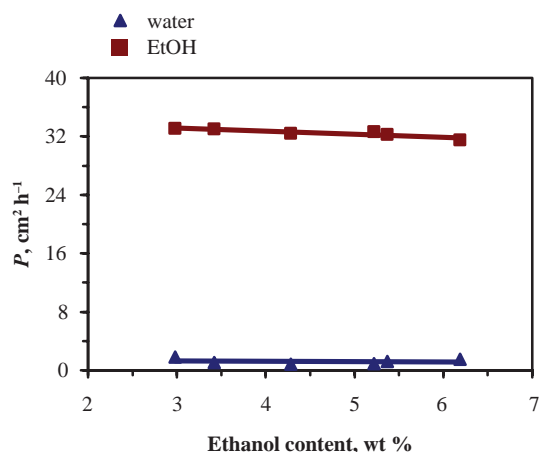


Fig. 4. Permeability coefficients of water and ethanol as a function of ethanol content in the broth.

increasing of free volume available for permeating molecules. The polymeric structure, consisting of an inorganic backbone and surrounded by methyl groups, influences the hydrophobicity of PDMS. The hydrogen bonds between permeant molecules and polymer are not allowed, only van der Waals interactions are possible.

The comparison of values of permeability coefficients indicates the preferential transport of ethanol across the membrane – an average ratio of P_B/P_A is close to 25 (Table 1). High permeability of ethanol is dominated mainly by sorption of this compound in PDMS. The ratio P_B/P_A is higher than observed selectivity coefficient α being within a range 7–9 and it can be considered as a measure of difference in component permeabilities at a lack of interactions between permeating molecules, i.e. for transport of pure components. The tendency to decrease of permeability coefficient of ethanol with ethanol content in the broth (Fig. 4), may be connected with increase of the content of organic compounds, i.e. glycerol, produced by the yeast under anaerobic conditions. These compounds of low polarity decrease the sorption of ethanol into a hydrophobic membrane. This correlation is observed for experiments with broth produced after 96 h of fermentation when the productivity of bioreactor stabilizes. In an earlier phase of fermentation the yeast cells in biocatalyst rapidly grows what determines the composition of the broth.

The values of plasticization coefficients of ethanol τ_B are higher than these of water (τ_A) for all experiments – contrary to expectations (Table 1). This fact indicates higher diffusivity of water due to the difference in size and structure of molecules. Plasticization coefficient of components show increasing tendency with ethanol content in the broth (Fig. 5). This dependency might

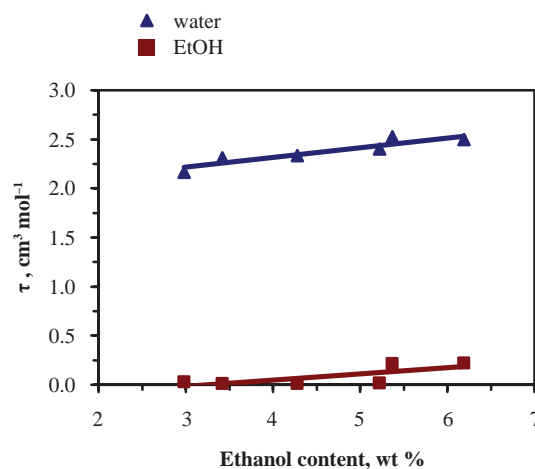


Fig. 5. Plasticization coefficients of water and ethanol as a function of ethanol content in the broth.

be explained by the sorption of organic compounds of larger molecules than ethanol, what generates the free volume for permeation and increases the plasticization degree of the polymer.

The values of coupled plasticization coefficients τ_{AB} , τ_{BA} point to a conclusion, that the promoting effect of ethanol for diffusivity of water is higher than the opposite effect (Table 1). These parameters are found to be independent on ethanol content in the broth ($R^2 < 0.4$). Thus coupled plasticization coefficients provide very specific information about the interactions of permeating components and polymer chains.

5. Conclusions

In this paper the application of the solution–diffusion theory for describing pervaporative separation of ethanol produced by the fermentation method was presented. Results of modeling of the process allowed to formulate the following conclusions.

1. A non-stationary model intended for description of the kinetics of ethanol separation has been formulated and tested. The model with four plasticization coefficients allows for obtaining very good agreement between experimental data and model predictions ($R^2 = 0.9998$ and higher).
2. The difference in permeability coefficients of water and ethanol indicates the fast transport of ethanol resulted from its preferential sorption in the hydrophobic polymer. The changes of permeability coefficients with the ethanol content in the broth are probably connected with the increase of concentration of other metabolites produced by the yeast.

3. The comparison of the values of plasticization coefficients of water and ethanol leads to conclusion that the difference in size and structure of molecules results in higher diffusivity of water.
4. Coupled plasticization coefficients can be considered as additional parameters characterizing interactions of transported compounds and a polymer due to their independence on feed composition.

Symbols

A_m	membrane area, m^2
C_i	concentration of permeant i , $mol \cdot m^{-3}$
D_i	diffusion coefficient of component i , $m^2 \cdot h^{-1}$
D_r	recovery coefficient of ethanol
J_i	flux of permeant i , $kg \cdot m^{-2} \cdot h^{-1}$
k_i	partition coefficient of permeant i
l	distance, m
m	mass, kg
P_i	permeability coefficient of permeant i , $m^2 \cdot h^{-1}$
R	correlation coefficient
RPDM	relative percentage deviation modulus, %
q	ratio of fluxes
s	standard deviation
t	time, h
w_i	weight fraction of component i
x_i	molar fraction of component i

Greek letters

α	Selectivity
Δ	thickness of a membrane, m
ε	pre-set value in the Nelder–Mead method
ϕ_i	sorption coefficient of component i
γ_i	activity coefficient of component i
ρ	density, $kg \cdot m^{-3}$
τ	plasticization coefficient, $m^2 \cdot mol^{-1}$

Indexes

A	Water
B	Ethanol
i	Component
j	Component
f	Feed
m	Membrane
p	Permeate

References

- [1] K.W. Böddeker, Terminology of pervaporation, *J. Membr. Sci.*, 51 (1990) 259–272.
- [2] J. Néel, Introduction to pervaporation, in: R.Y.M. Huang (Ed.), *Pervaporation Membrane Separation Processes*, Elsevier B.V., Amsterdam, 1991, pp. 1–81.
- [3] W. Kujawski, Application of pervaporation and vapor permeation in environmental protection, *Pol. J. Environ. Stud.*, 9 (2000) 13–26.
- [4] M. Lewandowska and W. Kujawski, Ethanol production from lactose in a fermentation/pervaporation system, *J. Food Eng.*, 79 (2007) 430–437.
- [5] M. Staniszewski, W. Kujawski and M. Lewandowska, Semi-continuous ethanol production in bioreactor from whey with co-immobilized enzyme and yeast cells followed by pervaporative recovery of product – Kinetic model predictions considering glucose repression, *J. Food Eng.*, 91 (2009) 240–249.
- [6] W. Kujawski, A. Warszawski, W. Ratajczak, T. Porebski, W. Capała and I. Ostrowska, Removal of phenol from wastewater by different separation techniques, *Desalination*, 163 (2004) 287–296.
- [7] M. Sekino, Study of an analytical model for hollow fiber reverse osmosis module systems, *Desalination*, 100 (1995) 85–97.
- [8] M.E. Williams, J.A. Hestekin, C.N. Smothers and D. Bhattacharyya, Separation of organic pollutants by reverse osmosis and nanofiltration membranes: mathematical models and experimental verification, *Ind. Eng. Chem. Res.*, 38 (1999) 3683–3695.
- [9] B. Wendler, B. Goers and G. Wozny, Regeneration of process water containing surfactants by nanofiltration – investigation and modelling of mass transport, *Water Sci. Technol.*, 46 (2002) 287–292.
- [10] P. Silva and A.G. Livingston, Effect of concentration polarisation in organic solvent nanofiltration – flat sheet and spiral wound systems, *Desalination*, 199 (2006) 248–250.
- [11] A.G. Koros and A.G. Fleming, Membrane-based gas separation, *J. Membr. Sci.*, 83 (1993) 1–83.
- [12] H.-Y. Yen and M.-H. Yang, Modified solution–diffusion model analysis of the flue gas desulfurization effluents in a polyamide membrane, *Polym. Test.*, 22 (2003) 109–113.
- [13] P. Schaetzel, C. Vauclair, G. Luo and Q.T. Nguyen, The solution–diffusion model: order of magnitude calculation of coupling between the fluxes in pervaporation, *J. Membr. Sci.*, 191 (2001) 103–108.
- [14] B. Cao and M.A. Henson, Nonlinear parameter estimation for solution–diffusion models of membrane pervaporation, *Ann. N. Y. Acad. Sci.*, 984 (2003) 370–385.
- [15] H.K. Lonsdale, U. Merten and R.L. Riley, Transport properties of cellulose acetate osmotic membranes, *J. Appl. Polym. Sci.*, 9 (1965) 1341–1362.
- [16] M.N. de Pinho, R. Rautenbach and C. Herion, Mass transfer in radiation-grafted pervaporation membranes, *J. Membr. Sci.*, 54 (1990) 131–143.
- [17] J. Stoer and R. Bulirsh, *Introduction to Numerical Analysis*, Springer-Verlag, New York-Heidelberg-Berlin, 1983.
- [18] T. Kreglewski, T. Rogowski, A. Ruszczynski and J. Szymanski, *Optimization Methods in FORTRAN*, PWN, Warszawa, 1984. (in Polish).